OPTIMAL PARAMETER DESIGN OF MULTIPLE TUNED MASS DAMPER FOR TALL BUILDINGS USING MULTI-OBJECTIVE PARTICLE SWARM OPTIMIZATION ALGORITHM CONSIDERING SOIL-STRUCTURE INTERACTION EFFECTS

DESENHO ÓTIMO DE PARÂMETROS DE UM AMORTECEDOR DE MASSA SINTONIZADO MÚLTIPLO PARA EDIFÍCIOS ALTOS UTILIZANDO UM ALGORITMO DE OTIMIZAÇÃO DE ENXAME DE PARTÍCULAS MULTIOBJETIVO CONSIDERANDO OS EFEITOS DA INTERAÇÃO SOLO-ESTRUTURA

DISEÑO ÓPTIMO DE PARÁMETROS DE UN AMORTIGUADOR DE MASAS SINTONIZADO MÚLTIPLE PARA EDIFICIOS ALTOS UTILIZANDO UN ALGORITMO DE OPTIMIZACIÓN DE ENJAMBRE DE PARTÍCULAS MULTIOBJETIVO QUE CONSIDERA LOS EFECTOS DE INTERACCIÓN SUELO-ESTRUCTURA

Reza Sobhanian
ORCID 0009-0004-8799-1341

Department of Civil Engineering, Tabriz Branch
Islamic Azad University
Tabriz, Iran

Rouzbeh Dabiri
ORCID 0000-0002-1807-1945

Department of Civil Engineering, Tabriz Branch
Islamic Azad University
Tabriz, Iran

Jamshid Sabouri*
ORCID 0000-0001-5512-5220

Department of Civil Engineering, Tabriz Branch
Islamic Azad University
Tabriz, Iran
J-Sabouri@iaut.ac.ir
* Correspond Author

Abstract. This study focuses on controlling structural vibrations during earthquakes by utilizing tuned mass dampers (TMD) to minimize structural responses. The optimization of damper parameters is crucial for achieving this goal. The research explores the use of multiple tuned mass dampers (MTMD) in place of a single TMD in the roof story. The impact of soil-structure interaction (SSI) on seismic responses is considered, necessitating an investigation into optimizing damper characteristics across different floors. Equations of motion for structures with multiple dampers and SSI were developed, and the state-space method was employed for solving these equations. Generalized mass and stiffness matrices for structures with MTMD and SSI were presented. The study utilized the multiple objective particle swarm optimization (MOPSO) algorithm to determine optimal damper parameters. The parameters of these dampers should be determined in such a way that they lead to minimum seismic responses of the structure. By analyzing 40-story benchmark and 20-story structures, the research highlights the significant influence of SSI on the distribution and stiffness of dampers within the structures, emphasizing the importance of considering interaction effects in damper optimization.

Keywords: Optimum design, Particle swarm optimization, Tuned mass dampers, Vibration control, Soil-structure interaction, Multiple tuned mass dampers.

Resumo. Este estudo concentra-se no controle das vibrações estruturais durante terremotos por meio do uso de amortecedores de massa sintonizados (TMD), visando minimizar as respostas estruturais. A otimização dos parâmetros dos amortecedores é fundamental para alcançar esse objetivo. A pesquisa explora o uso de múltiplos amortecedores de massa sintonizados (MTMD) em vez de um único TMD localizado no topo do edifício. Considera-se o impacto da interação solo-estrutura (SSI) nas respostas sísmicas, o que exige uma investigação detalhada para otimizar as características dos amortecedores em diferentes pavimentos. Equações de movimento foram desenvolvidas para estruturas com múltiplos amortecedores e SSI, sendo resolvidas por meio do método de espaço de estados. Matrizes de massa e rigidez generalizadas foram apresentadas para estruturas com MTMD e SSI. O estudo utilizou o algoritmo de otimização de enxame de partículas multiobjetivo (MOPSO) para determinar os parâmetros ideais dos amortecedores. Esses parâmetros devem ser definidos de maneira a minimizar as respostas sísmicas da estrutura. Analisando estruturas de referência com 40 e 20 andares, a pesquisa destaca a influência significativa da

SSI na distribuição e rigidez dos amortecedores dentro das estruturas, enfatizando a importância de considerar os efeitos de interação na otimização dos amortecedores.

Palavras-chave: Desenho ótimo, Otimização de enxame de partículas, Amortecedores de massa sintonizados, Controle de vibrações, Interação solo-estrutura, Amortecedores de massa sintonizados múltiplos.

Resumen. Este estudio se centra en el control de las vibraciones estructurales durante los terremotos mediante el uso de amortiguadores de masa sintonizados (TMD) para minimizar las respuestas estructurales. La optimización de los parámetros de los amortiguadores es crucial para lograr este objetivo. La investigación explora el uso de múltiples amortiguadores de masa sintonizados (MTMD) en lugar de un solo TMD en el piso del techo. Se considera el impacto de la interacción suelo-estructura (SSI) en las respuestas sísmicas, lo que requiere una investigación para optimizar las características de los amortiguadores en diferentes pisos. Se desarrollaron ecuaciones de movimiento para estructuras con múltiples amortiguadores y SSI, y se empleó el método de espacio de estados para resolver estas ecuaciones. Se presentaron matrices de masa y rigidez generalizadas para estructuras con MTMD y SSI. El estudio utilizó el algoritmo de optimización de enjambre de partículas de múltiples objetivos (MOPSO) para determinar los parámetros óptimos de los amortiguadores. Los parámetros de estos amortiguadores deben determinarse de tal manera que conduzcan a respuestas sísmicas mínimas de la estructura. Al analizar estructuras de referencia de 40 pisos y de 20 pisos, la investigación destaca la influencia significativa de SSI en la distribución y rigidez de los amortiguadores dentro de las estructuras, enfatizando la importancia de considerar los efectos de interacción en la optimización de los amortiguadores.

Palabras-clave: Diseño óptimo, Optimización de enjambre de partículas, Amortiguadores de masa ajustados, Control de vibraciones, Interacción suelo-estructura, Amortiguadores de masa ajustados múltiples.

1. INTRODUCTION

The need to control vibrations in tall buildings and structures to mitigate potential damages has become increasingly crucial. Research in the field of reducing vibrations caused by earthquakes or winds through active or passive control systems has been further pursued. While active control systems are often deemed less preferable due to economic and safety concerns, passive control systems like tuned mass damper (TMD) devices are considered advantageous (Bekdaş et al., 2019). However, meeting structural space requirements for TMD designs can pose challenges. Liu et al. explored this aspect by investigating the design of an economically feasible TMD using a genetic algorithm to reduce stroke (Liu et al., 2020).

Various studies have focused on designing TMDs economically by adjusting parameters to minimize structural system responses, with Artificial Intelligence methods like Artificial Neural Networks (ANN) being utilized for this purpose (Yucel et al., 2019). An analytical approach was developed to estimate TMD parameters, highlighting the benefits of utilizing an optimized viscoelastic TMD for enhanced flexibility and superior vibration reduction compared to viscously damped TMDs (Batou and S. Adhikari, 2019).

Significant changes in the dynamic responses of tall buildings are observed when considering soil-structure interaction (SSI) (Araz, 2022). Investigating the effect of SSI, assuming elastic behavior for the soil, on the seismic response of a 20-story steel structure with a reduced stiffness matrix of the foundation-soil-foundation system reveals a significant increase in the structure's responses (Fatollahpour et al., 2023).

Considering the SSI effect can lead to a reduction in the linear structural response of a building with an optimal Tuned Mass Damper (TMD) subjected to strong motion earthquakes (Salvi et al., 2018). Jia and Jianwen's (2019) study analyzed the performance of a TMD on the top of a structure while considering the SSI effect, highlighting a degradation in the TMD's performance when ignoring SSI. Additionally, an optimization problem with five objective functions was addressed to optimize structural responses with SSI, evaluating the performance of the objective functions (Araz et al., 2022). Several studies have focused on optimizing Tuned Mass Damper (TMD) parameters to reduce structural responses in buildings, yielding efficient results through the use of metaheuristic algorithms. These methods have proven effective in

fine-tuning TMD parameters, leading to significant reductions in structural responses. Etedali et al. investigated the performance of both TMD and Friction TMD (FTMD), a novel device combining traditional linear TMD with a friction damper, for controlling high-rise structures while considering soil-structure interaction (SSI) effects.

Their study utilized a multi-objective cuckoo search (MOCS) optimization algorithm to tune TMD and FTMD parameters, analyzing MOCS performance under various ground conditions (Araz et al., 2023; Shahraki et al., 2023; Vanshaj et al., 2022; Kayabekir et al., 2022; Lara-Valencia et al., 2022; Djerouni et al., 2022; Fahimi Farzam & A. Kaveh, 2020; Brandão & Miguel 2020; Bekdaş et al., 2018).

The main contribution of this paper is to present an optimized parameter design of Multiple Tuned Mass Dampers (MTMDs) considering Soil-Structure Interaction (SSI) effects in soft soil and fixed base cases, applied to two example buildings. The objective is to minimize roof acceleration and displacement in the analyzed buildings. For both case studies, the widely-used Multi-objective Particle Swarm Optimization (MOPSO) algorithm is employed to optimize the two objective functions mentioned earlier.

The study compares and evaluates the optimal designs for structures without and with SSI effects, featuring TMDs installed on all stories. The stiffness and mass of the TMDs is determined by the MOPSO algorithm, with optimal solutions selected at the result of the MOPSO iterations.

2. METHOD

2.1. Soil-structure interaction with TMD system optimization problem

As stated the objective of this study is to propose an optimal MTMD design, wherein the stiffness and mass of TMDs serve as decision variables to be optimized using the MOPSO algorithm while considering SSI effects. The primary goal of this optimization is to minimize both the maximum acceleration and displacement of the roof in the target structures. Thus, the problem is formulated as a multi-objective optimization task with two objective functions: maximum acceleration and maximum roof displacement. The damping characteristics of TMDs were determined using the Rayleigh method (Thomson, 2018). All structures investigated in this paper were subjected to the El-Centro earthquake. Mathematically, the optimization problem addressed in this study can be expressed as follows:

$$Find: (M_{TMD})_h, (K_{TMD})_h : h = 1, \dots, N,$$
$$Minimize: max(|X_i(t)|, |A_i(t)|) \ : t = 1,2, \dots, t_{max}, i = 1,2, \dots, N \qquad (1)$$

In the equation, h represents the number of stories where a TMD is installed, t denotes time, and N stands for the maximum number of stories. Xi and Ai represent the displacement and acceleration of the ith story, respectively. For this analysis, i was set equal to N as we aim to examine the maximum displacement and acceleration of the roof. MTMD and KTMD indicate the mass and stiffness of the TMD, respectively

In order to calculate the responses resulted from earthquake in two shear buildings considered in this paper, which use TMDs placed in each story and also SSI effects, a theoretical model is presented and shown in figure 1. The equation of motion by considering SSI in a shear building with MTMD is developed as follows:

$$[M]\ddot{X}(t) + [C]\dot{X}(t) + [K]X(t) = -[m^*]\ddot{X}_g, \qquad (2)$$

[M], [C], [K] and [m*] indicate the mass, damping, stiffness and acceleration mass matrices of the considered systems. Here, $\ddot{X}(t)$, $\dot{X}(t)$ and $X(t)$ show acceleration, velocity and displacement vectors of the presented structural system being analyzed. These matrices can be mathematically expressed as equations (3)- (8):

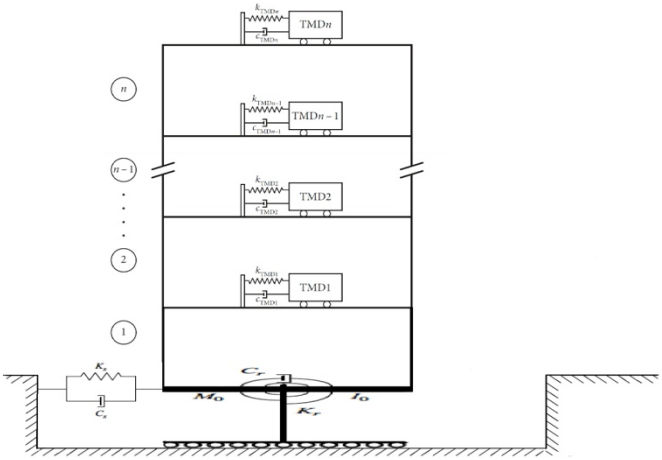

Figure 1. Model of Multiple TMDs with SSI effects in shear buildings.

$$[K]=\begin{bmatrix} K_1+K_2+K_{TMD1} & -K_2 & \dots & 0 & -K_{TMD1} & 0 & \dots & 0 & 0 & 0 \\ -K_2 & K_2+K_3+K_{TMD2} & \dots & 0 & 0 & -K_{TMD2} & \dots & 0 & \vdots & \vdots \\ \vdots & \vdots & \ddots & \vdots & \vdots & \vdots & \dots & \vdots & \vdots & \vdots \\ 0 & 0 & \dots & K_n+K_{TMDn} & 0 & 0 & \dots & -K_{TMDn} & \vdots & \vdots \\ -K_{TMD1} & 0 & \dots & 0 & K_{TMD1} & 0 & \dots & 0 & \vdots & \vdots \\ 0 & -K_{TMD2} & \dots & 0 & 0 & K_{TMD2} & \dots & 0 & \vdots & \vdots \\ \vdots & \vdots & \ddots & \vdots & \vdots & \vdots & \ddots & \vdots & \vdots & \vdots \\ 0 & 0 & \dots & -K_{TMDn} & 0 & 0 & \dots & K_{TMDn} & 0 & \vdots \\ 0 & \dots & \dots & \dots & \dots & \dots & \dots & 0 & K_s & 0 \\ 0 & \dots & \dots & \dots & \dots & \dots & \dots & \dots & 0 & K_r \end{bmatrix} \quad (3)$$

$$[M]=\begin{bmatrix} [M_{structure}] & [M_V] & [MZ] \\ [M_V]^T & M_0+\sum_{j=1}^{N} M_j+\sum_{j=1}^{N} M_{dj} & \vdots \\ [MZ]^T & \dots & I_0+\sum_{i=1}^{N} I_i+(\sum_{i=1}^{N} m_{di}Z_i^2)+(\sum_{i=1}^{N} m_iZ_i^2) \end{bmatrix} \quad (4)$$

$$[M_V]=\begin{bmatrix} m_1 \\ m_2 \\ \vdots \\ m_n \\ m_{d1} \\ \vdots \\ m_{dn} \end{bmatrix} \quad (5)$$

$$[MZ] = \begin{bmatrix} m_1 z_1 \\ m_2 z_2 \\ \vdots \\ m_n z_n \\ m_{d1} z_1 \\ \vdots \\ m_{dn} z_n \end{bmatrix} \quad (6)$$

$$[m^*] = \begin{bmatrix} m_1 \\ m_2 \\ \vdots \\ m_n \\ m_{d1} \\ m_{d2} \\ \vdots \\ m_{dn} \\ m_0 + \left(\sum_{i=1}^{N} m_i\right) + \left(\sum_{i=1}^{N} m_{di}\right) \\ \sum_{i=1}^{N} m_i z_i + \sum_{i=1}^{N} m_{di} z_i \end{bmatrix} \quad (7)$$

$$x(t) = \begin{bmatrix} x_1 \\ x_2 \\ \vdots \\ x_n \\ x_{d1} \\ \vdots \\ x_{dn} \\ x_0 \\ \theta_0 \end{bmatrix} \quad (8)$$

The damping matrix can be formulated using the Rayleigh method as presented in Thamson (2018). In the presented matrices, Kn is the stiffness of the nth story, $(K_{TMD})_n$ is the stiffness of TMD in the nth story, Ks and Kr are swaying stiffness and rocking stiffness coefficients, respectively, Mstructure is the mass matrix of the structure, Mn and Mdn are the mass of the nth story and mass of the TMD placed in the nth story, respectively, M0 is the mass of the foundation, I0 is the moment of inertia of the foundation, Zi denotes the location of the ith story, xi shows the displacement of the ith story and xdi indicates the displacement of the ith TMD. X0 and θ0 are the displacement and rotation of the base, respectively. State-space method was used in order to solve the equations of motions for the provided examples.

The motioned equation can be represented in terms of state-space method, as follows (Ogata, 2010):

$$Z(t) = AZ(t) + BU(t), \quad (9)$$

$$Y(t) = RZ(t) + QU(t), \quad (10)$$

$$\dot{X}(t) \quad (11)$$

Where A and B matrices can be defined as follows:

$$\begin{bmatrix} -M^{-1}K & -M^{-1}C \end{bmatrix} \quad (12)$$

$$\begin{bmatrix} -M^{-1}m^{*} \end{bmatrix} \quad (13)$$

Y(t) is the output vector, can be considered as acceleration, displacement or velocity of structural system.

2.2. Multi objective particle swarm Optimization algorithm

To address multiple objectives in optimization problems, extending single-objective optimization methods like evolutionary algorithms appears promising. This approach is particularly viable because certain single-objective optimization algorithms, such as the Particle Swarm Optimization (PSO) algorithm, demonstrate fast convergence when solving single-objective optimization tasks (Kennedy & Eberhart, 1995). This extension generally allows the algorithm to optimize multiple objective functions in optimization problems where more than one function needs optimization. For this reason, a multi-objective particle swarm optimization algorithm was utilized to solve the optimization problem considered in this paper, which involves two objective functions: the maximum acceleration value at the roof and the maximum displacement value at the roof in two high-rise buildings with 20 and 40 stories. The research results show that MOPSO is an effective method in solving multi-objective optimization problems, which is also used in this article (Coello et al., 2004).

Based on the fact that PSO can be efficiently utilized for solving the problems defined in the next section of this paper, owing to the high convergence ratio of PSO in solving single-objective optimization problems (Kennedy & Eberhart, 1995). Therefore, the performance of its multi-objective version was put to the test in dealing with the defined optimization problems. PSO consists of search agents that change their position in iterations to explore and exploit different regions of the optimization problem. In fact, each search agent also has a position and velocity vector, which can be mathematically represented as follows:

$$X_i^t = \{X_{i1}^t, X_{i2}^t, \dots, X_{in}^t\} \quad (14)$$

$$V_i^t = \{V_{i1}^t, V_{i2}^t, \dots, V_{in}^t\} \quad (15)$$

Where i is the ith particle, t is the current iteration, X denotes a position vector, n indicates the number of decision variables and V is a velocity vector. In the search space of the optimization problem, these particles are capable of movement and adjusting their positions according to their updated velocities. During each iteration, two particles were identified as the best-position particle and the global best position among the areas visited by the particles.

$$\vec{V}_i^{t+1} = \omega^t \vec{V}_i^t + C_1 r_1 \left(pbest_i^t - \vec{X}_i^t\right) + C_2 r_2 \left(gbest^t - \vec{X}_i^t\right) \quad (16)$$

Where pbest is the best position particle, gbest is the global best position, ωt is the inertia weight, r1 and r2 are two random numbers in the interval of zero and one and C1 and C2 are considered as cognitive and social scaling values, respectively.

The position vector can be mathematically expressed as follows:

$$\vec{X}_i^{t+1} = \vec{X}_i^t + \vec{V}_i^{t+1} \quad (17)$$

The values for ωt, C1 and C2 are assumed to be 0.5, 1 and 2, respectively for all of the numerical examples considered in this paper. The inertia weight plays an essential role in generating efficient candidate solutions for optimization problems. Therefore, altering its value through another parameter, known as the inertia weight damping rate, over the iterations of the PSO algorithm can influence the solutions of optimization problems. The inertia weight can be defined as follows

$$\omega^{t+1} = \omega^{t} \times \omega_{Damp} \quad (18)$$

The value for ωDamp in this study is set to 0.99. The number of search agents and maximum number of iterations are set to 100 and 100, respectively. To conduct a statistical analysis on the results obtained for each of the shear buildings under consideration, each structure was optimized by MOPSO in 10 independent optimization runs. Three Pareto fronts were reported for each structure, and one of them was selected to demonstrate the results.

2.3. Numerical examples

To investigate the effects of SSI on structures with multiple TMDs placed in each story, two structures were considered in this study. A 40-story shear building with soft soil and a fixed base condition, as presented in (Coello et al., 2004; Liu et al., 2008), was examined. Another shear building with 20 stories under both soft soil and fixed base conditions was also analyzed. These structures were optimized using MOPSO, and the results were presented. The properties of the analyzed structures can be found in Table 1.

Table 1. The parameters of 40 story shear building.

Parameter	Value
Height of Story (m)	4
Mass of story (kg)	9.8×10^{5}
Inertia moment of story (kg.m2)	1.31×10^{8}
Stiffness of story (N/m)	K1 =2.31×10^{9} –K_{40}=9.98×10^{8}
Mass of foundation (kg)	1.96×10^{6}
Inertia moment of foundation (kg.m2)	1.96×10^{8}

Table 2. Soil and foundation parameters for soft soil.

Kr (N.S/m)	Ks (N.s/m)	Cr (N/m)	CS (N.s/m)
7.53×10^{11}	1.91×10^{9}	2.26×10^{10}	2.19×10^{8}

The mass and stiffness lower bounds and upper bounds of TMDs in each story of the 40-story shear building were specified in table 3. The lower and upper bounds of stiffness for TMDs were selected from (Khatibinia et al., 2016), but the lower and upper bounds of mass parameter for TMDs were assumed to be between 0.01 and 0.1 of story mass.

Table 3. Lower bounds and upper bounds of TMDs parameters for 40 story building.

Parameter of TMD	Lower bound	Upper bound
MTMD (kg)	9800	98000
KTMD (N/m)	0.5e+06	60e+06

Tables 1 and 2 were also applied for the 20-story shear building, except that the stiffness of stories ranged from K1=1.63×109 – K40=9.98×108. Table 3 was also used without being

changed for the 20-story shear building. Figure 2 depicts the accelerogram to which both of the considered structures were subjected (Khatibinia et al., 2016).

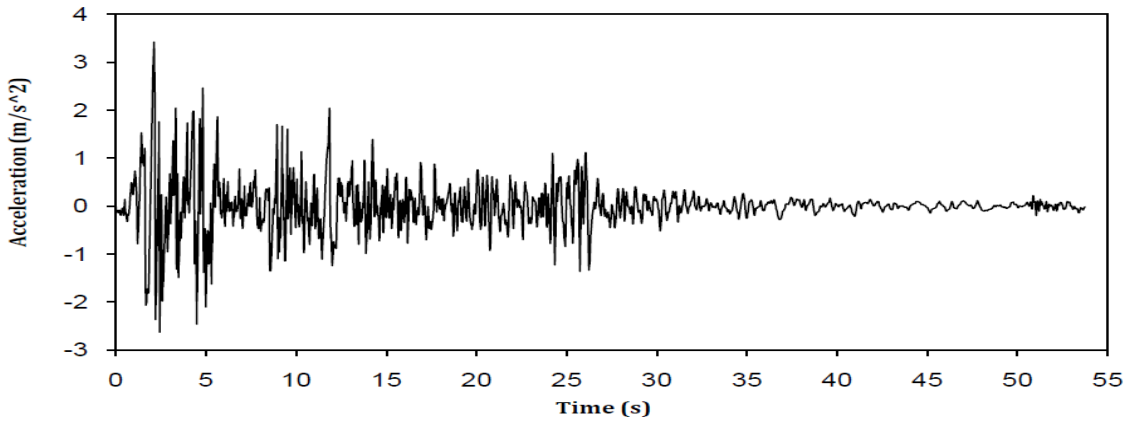

Figure 2. Accelerogram of the El–Centro earthquake.

2.4. TMD Optimization of 40 Story Frame of benchmark

The work in the article (Khatibinia et al., 2016) of a 40-story shear building that was equipped with a single damper on the roof floor had been optimized with the MOPSO algorithm, considering the effects of soil-structure interaction (SSI). In this research, the same 40-story structure from article (Khatibinia et al., 2016) was modeled by maintaining the details and characteristics of the structure and the soil, but dampers were placed in all floors instead of only on the roof floor. The parameters of all dampers were optimized until the minimum responses (acceleration and displacement of the roof story) were achieved.

For this purpose, mass and stiffness matrices were first developed for the multi-damper structure with soil-structure interaction (SSI), and then optimization was carried out. The seismic response of the structure was analyzed after optimization. To confirm the obtained results, the same procedure was conducted for the 20-story shear building.

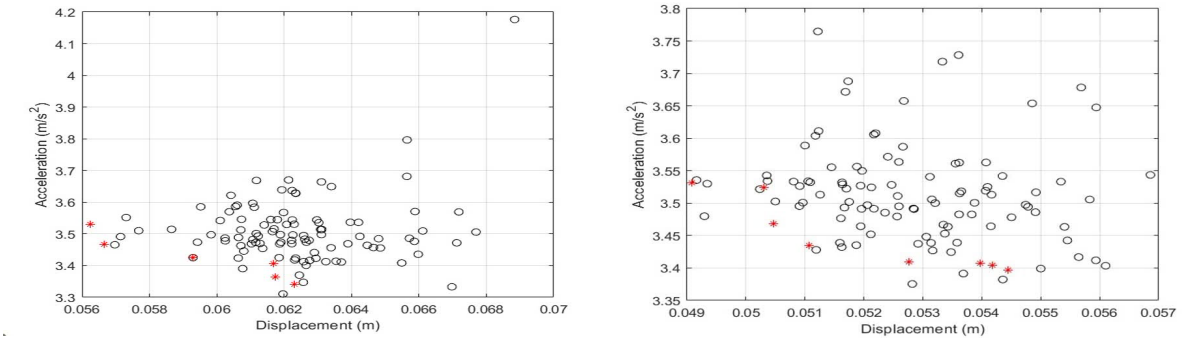

(a) fixed based (b) with SSI

Figure 3. Pareto optimal frontier for 40 story building.

Figures 3a and 3b show the Pareto front diagrams for the optimal design of a 40-story building with fixed support (without soil-structure interaction) and with soil-structure interaction, respectively, where the optimized responses are marked with asterisks (Pareto front diagrams). For discussion and investigation, three items were selected as the optimal response from all the optimized responses in the graphs.

The design results for each of the three optimal responses selected are reported in Table 4, which includes the total mass of TMDs distributed in the stories, the ratio of the mass of TMDs to the total mass of the structure, the period of the structure, the maximum acceleration and displacement of the roof story. Upon studying Table 4, it is evident that in the 40-story structure (with and without interaction), the results of all three fronts are closely aligned. Therefore, for each structure among the three fronts, only one front was selected, and the study proceeded with it.

Table 4. Optimal values for TMDs of 40 story shear building fixed base and SSI.

Parameters	Multi TMD- fixed base				Multi TMD-SSI		
	front1	front2	front3		front1	front2	front3
Mass of Structure (ton)	39200	39200	39200		39200	39200	39200
SUM of TMDs Mass (ton)	2324	2316	2318		2283	2295	2264
Mass percentage of TMDs (%)	5.93	5.91	5.91		5.82	5.85	5.78
Time Period (s)	3.83	3.83	3.83		4.39	4.39	4.39
Displacement of roof (cm)	5.90	5.60	6.10		5.10	5.40	4.90
Acceleration of roof (m/s2)	3.43	3.46	3.41		3.43	3.40	3.53

The analysis results of the 40-story benchmark structure (Khatibinia et al., 2016) are presented in Table 5, considering two scenarios: one with a single damper installed in the roof story under soil-structure interaction, and the other involving the distribution of dampers across the stories, both with and without interaction effects. It is important to highlight that, from the three responses outlined in Table 4, the optimal response was chosen for the damper distribution across the stories, and the corresponding results are provided.

Upon reviewing the results presented in Table 5 (columns one and three), a significant improvement is observed when employing Multiple Tuned Mass Dampers (MTMD) instead of a single TMD. In the case of the 40-story benchmark structure, the utilization of multiple dampers (columns one and three) led to notable reductions in structural responses, specifically a decrease in acceleration from 4.38 to 3.53 and a decrease in displacement from 25 to 4.9. Furthermore, an examination of columns two and three of Table 5 reveals that the 40-story structures equipped with multi-dampers, irrespective of interaction effects, demonstrate minimal seismic responses, owing to the optimization of mass distribution and damper stiffness.

Table 5. Optimal values for TMDs of 40 story (fixed based and SSI) for a selected Pareto front

Parameters	One TMD at roof -SSI	Multi TMD- fixed base	Multi TMD-SSI
Mass of Structure (ton)	39200	39200	39200
SUM of TMDs Mass (ton)	258	2316	2264
Mass percentage of TMDs (%)	0.72	5.91	5.78
Time Period (s)	4.48	3.83	4.39
Displacement of roof (cm)	25.00	5.60	4.90
Acceleration of roof (m/s2)	4.38	3.46	3.53

In these figures, it is evident that the interaction between soil and structure significantly impacts the distribution of mass and stiffness of dampers within the stories of the structure, resulting in different design outcomes. Figure 4 depicts the mass distribution of dampers across the height of the 40-story structure. The maximum mass of the dampers in the non-interaction state (40-story MTMD-fixed) occurred on stories 7, 12, 15, 30, and 31. However, after the interaction of these stories, the minimum mass of the dampers was observed. Furthermore, the

minimum mass of the dampers in the non-interaction state (40-story MTMD-fixed) was found in stories 1, 14, 20, 32, and 38, but after the interaction was applied, these stories had the maximum mass of dampers.

Figure 5 displays the stiffness distribution of the dampers at the height of the structure. Similar to the mass distribution, the results vary significantly due to the interaction between the soil and structure.

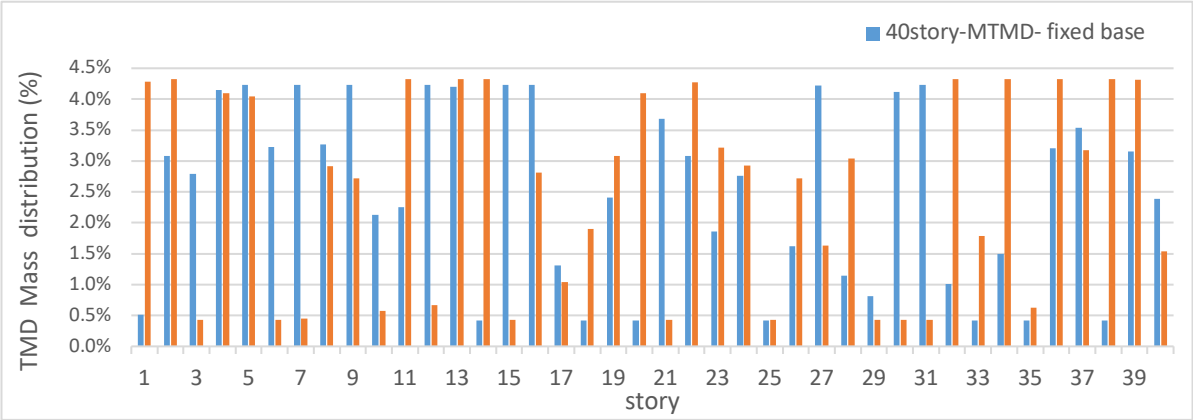

Figure 4. TMD Mass distribution in stories for 40 story fixed base and SSI

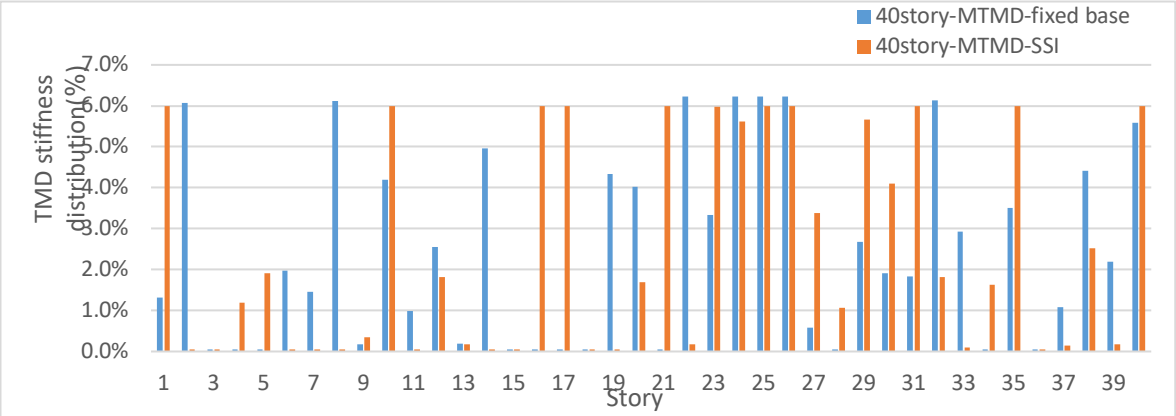

Figure 5. TMD stiffness distribution in stories for 40 story fixed base and SSI.

In this article, the distribution of mass and stiffness of dampers in the height of the stories of both models of the 40-story structure (with and without interaction) has been optimized in order to minimize seismic responses such as roof displacement and acceleration. In other words, the design of dampers in both structures has been carried out with the same objective of achieving acceptable and similar seismic responses.

Figures 6 and 7 show the acceleration and displacement of the roof story for the optimized models of dampers in both cases, with and without soil and structure interaction, having similar values. This result suggests that the structure design has reached convergence in both cases, with the only difference in the mass distribution and stiffness of the dampers being attributed to the effects of soil and structure interaction.

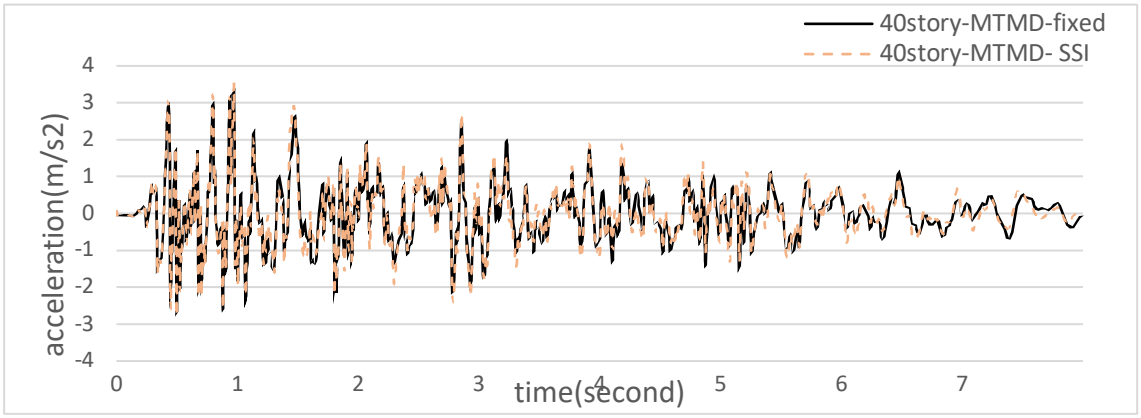

Figure 6. Time history acceleration of the top story for 40 story-MTMD (fixed base-SSI)

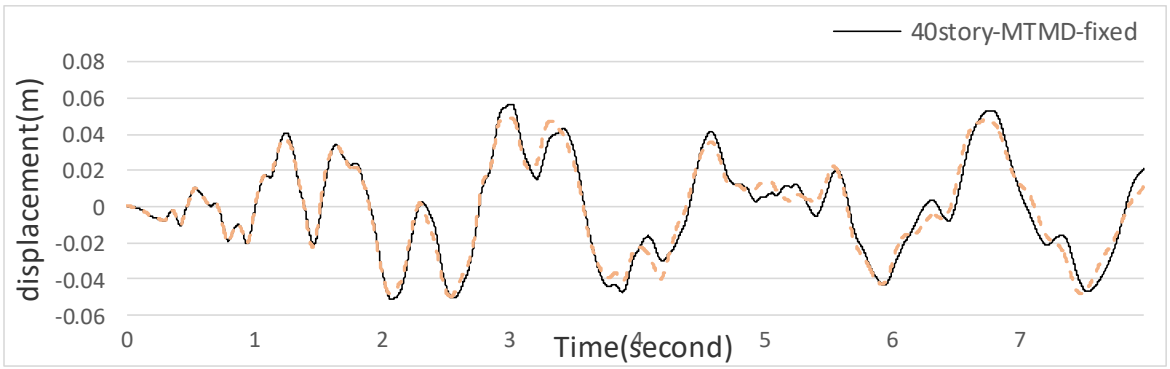

Figure 7. Time history displacement and acceleration of the top story for 40 story- SSI

2.5. TMD Optimization of 20 Story Frame

In order to verify and validate the perceptions of the previous sections (1-4), a 20-story building was modeled based on the specifications outlined in part 4. Once the analysis was finished, the optimal outcomes were showcased in the Pareto front diagram. Figures 8a and 8b display the Pareto front diagrams for the best design of a 20-story structure both with and without soil-structure interaction, with the optimized responses indicated by asterisks. Among all the marked responses in the diagram, three optimal answers for discussion and reviews have been selected.

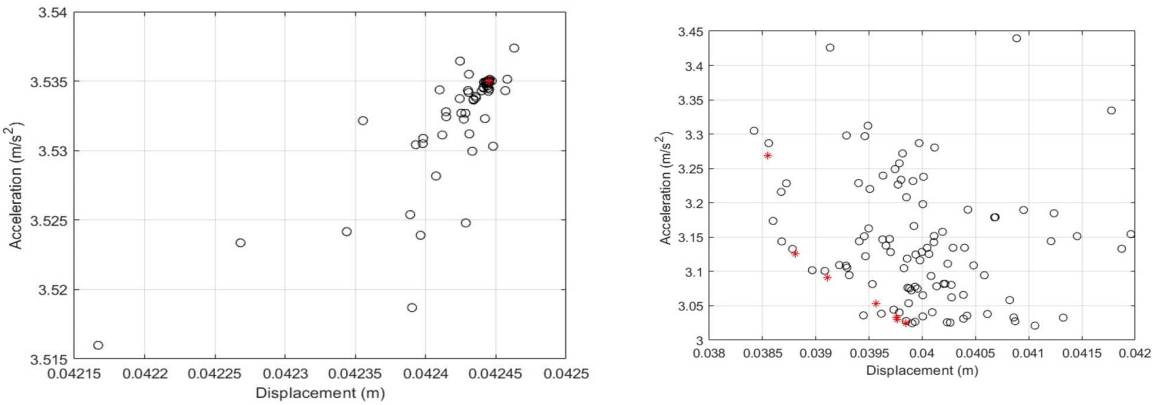

(a) fixed based (b) with SSI

Figure 8. Pareto optimal frontier for 20 story building.

The design results for each of the three optimal responses selected are reported in Table 6. This includes the total mass of Tuned Mass Dampers (TMDs) distributed in the stories, the ratio of the mass of TMDs to the total mass of the structure, the period of the structure, and the maximum acceleration and displacement of the roof story. By studying Table 6, it is evident that in the 20-story structure (with and without interaction), the results of all three fronts are similar. Therefore, only one front from the three was selected for further study on each state of the structure.

Table 6. Optimal values for TMDs of 20 story shear building fixed base and SSI.

Parameters	Multi TMD- fixed base				Multi TMD-SSI		
	front1	front2	front3		front1	front2	front3
Mass of Structure (ton)	19600	19600	19600		19600	19600	19600
SUM of TMDs Mass (ton)	1316	1316	1316		1569	1566	1586
Mass percentage of TMDs (%)	6.71	6.71	6.71		8.01	7.99	8.09
Time Period (s)	2.20	2.20	2.20		2.23	2.23	2.23
Displacement of roof (cm)	4.20	4.20	4.20		3.90	3.88	3.95
Acceleration of roof (m/s2)	3.53	3.53	3.53		3.033	3.125	3.053

An optimal response was selected for both states of the 20-story structure (with interaction and without interaction) from the three responses presented in Table 4. The corresponding results are provided in Table 7. After analyzing the results in Table 7, it is evident that the placement of mass dampers in 20-story structures, both with and without interaction, has been optimized to achieve seismic responses that are similar. The distribution of dampers was determined to yield minimal and acceptable seismic responses.

Table 7. Optimal values for TMDs of 20 story (fixed base and SSI) for a selected Pareto front

Parameters	Multi TMD- fixed base	Multi TMD-SSI
Mass of Structure (ton)	19600	19600
SUM of TMDs Mass (ton)	1316	1569
Mass percentage of TMDs (%)	6.71	8.01
Time Period (s)	2.20	2.23
Displacement of roof (cm)	4.20	3.90
Acceleration of roof (m/s2)	3.53	3.033

The results of optimizing and distributing mass and stiffness of Tuned Mass Dampers (TMDs) in a 20-story building are shown in Figures 11 and 12. This distribution of mass and stiffness in the stories is accomplished to minimize seismic responses (displacement and acceleration of the roof story) and demonstrates the optimal condition. In these figures, it is evident that the interaction between soil and structure significantly impacts the distribution of mass and stiffness of dampers in the stories of the structure, leading to different design outcomes. Figure 9 illustrates the distribution of damper mass in a 20-story structure with and without soil-structure interaction. Figure 10 depicts the stiffness distribution of the dampers at the height of the structure. The stiffness distribution, as with the mass, yields significantly different design outcomes when considering the interaction between the soil and structure.

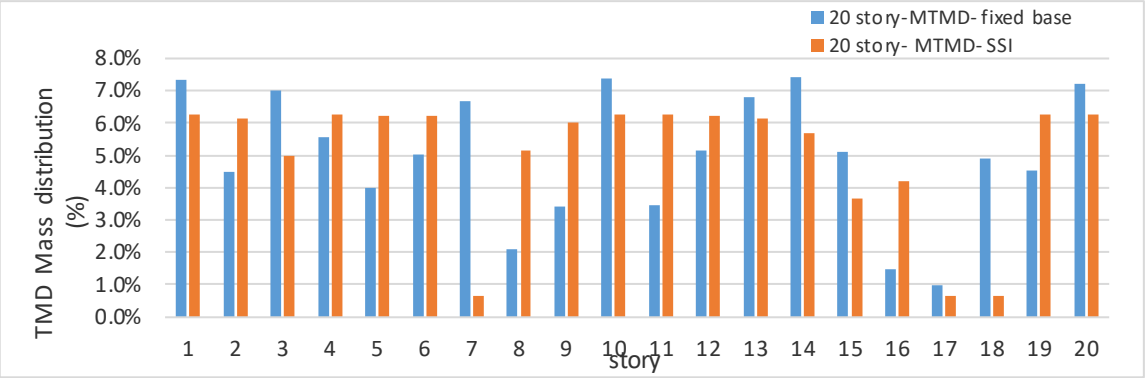

Figure 9. TMD Mass distribution in stories for 20 story fixed base and SSI.

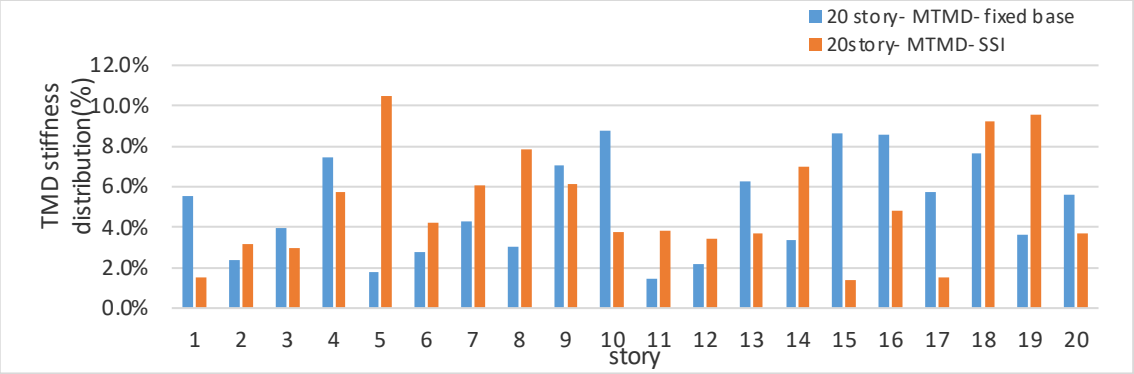

Figure 10. TMD stiffness distribution in stories for 40 story fixed base and SSI

Figures 11 and 12 show the acceleration and displacement of the roof floor for the optimized models of the dampers in both cases with and without the interaction of the soil - structure subjected to El-Centro earthquake, and the responses in both structures are nearly identical.

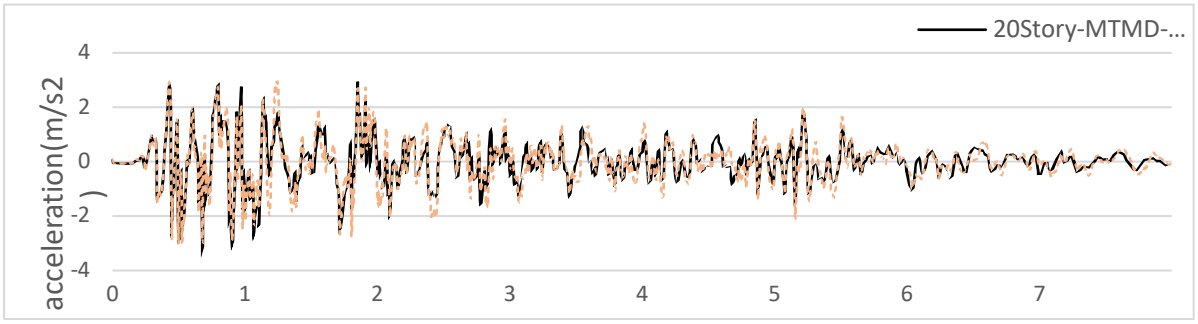

Figure 11. Time history acceleration of the top story for 20 story-MTMD (fixed base-SSI)

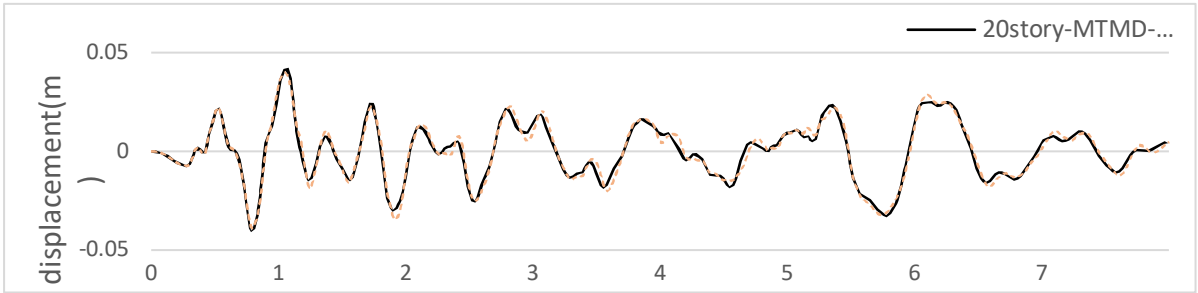

Figure 12. Time history displacement and acceleration of the top story for 20 story- SSI

Br. J. Ed., Tech. Soc., v.17, n.se3, p.216-230, 2024
DOI http://dx.doi.org/10.14571/brajets.v17.nse3.216-230
ISSN 2316-9907

3. CONCLUSION

In this paper, 40-story benchmark and 20-story structures with and without considering the interaction of soil and structure (SSI) were investigated in both single-damper and multi-damper states. The results indicate that:

Placing multiple optimized dampers in each story, rather than a single damper in the roof story, significantly reduces the seismic responses (acceleration and displacement of the roof story). The acceleration has been reduced from 4.38 to 3.53 m/s2 and displacement from 25 to 4.9 cm.

In the optimization of mass dampers in the stories using the MOPSO algorithm, minimal and similar seismic responses were achieved for both cases with and without soil and structure interaction.

Considering the interaction between the soil and structure significantly affects the distribution of dampers in the stories. This has resulted in changes to the amount of mass and stiffness assigned to the dampers in some stories, switching from maximum to minimum values and vice versa

REFERENCES

Araz, O. (2022). Optimization of tuned mass damper inerter for a high-rise building considering soil-structure interaction. Archive of Applied Mechanics, 92(10), 2951-2971.

Araz, O., Ozturk, K. F., & Cakir, T. (2022). Effect of different objective functions on control performance of tuned mass damper for a high-rise building considering soil–structure interaction. Archive of Applied Mechanics, 92(4), 1413-1429.

Araz, O., Elias, S., & Kablan, F. (2023). Seismic-induced vibration control of a multi-story building with double tuned mass dampers considering soil-structure interaction. Soil Dynamics and Earthquake Engineering, 166, 107765.

Batou, A., & Adhikari, S. (2019). Optimal parameters of viscoelastic tuned-mass dampers. Journal of Sound and Vibration, 445, 17-28.

Bekdaş, G., Kayabekir, A. E., Nigdeli, S. M., & Toklu, Y. C. (2019). Tranfer function amplitude minimization for structures with tuned mass dampers considering soil-structure interaction. Soil Dynamics and Earthquake Engineering, 116, 552-562.

Bekdaş, G., Nigdeli, S. M., & Yang, X. S. (2018). A novel bat algorithm based optimum tuning of mass dampers for improving the seismic safety of structures. Engineering Structures, 159, 89-98.

Brandão, F. D. S., & Miguel, L. F. F. (2020). Vibration control in buildings under seismic excitation using optimized tuned mass dampers. Frattura ed integrità strutturale [recurso eletrônico].[Frosinone, Itália]. Vol. 54 (Oct. 2020), p. 66-87.

Coello, C. A. C., Pulido, G. T., & Lechuga, M. S. (2004). Handling multiple objectives with particle swarm optimization. IEEE Transactions on evolutionary computation, 8(3), 256-279.

Djerouni, S., Abdeddaim, M., Elias, S., & Rupakhety, R. (2021). Optimum double mass tuned damper inerter for control of structure subjected to ground motions. Journal of Building Engineering, 44, 103259.

Fahimi Farzam, M., & Kaveh, A. (2020). Optimum design of tuned mass dampers using colliding bodies optimization in frequency domain. Iranian Journal of Science and Technology, Transactions of Civil Engineering, 44, 787-802.

Fatollahpour, A., Tafakori, E., & Arjmandi, S. A. A. (2023). The effects of structure-soil-structure

interaction on seismic response of high-rise buildings equipped with optimized tuned mass damper. In Structures (Vol. 50, pp. 998-1010). Elsevier.

Jia, F., & Jianwen, L. (2019). Performance degradation of tuned-mass-dampers arising from ignoring soil-structure interaction effects. Soil Dynamics and Earthquake Engineering, 125, 105701.

Kayabekir, A. E., Nigdeli, S. M., & Bekdaş, G. (2022). A hybrid metaheuristic method for optimization of active tuned mass dampers. Computer-Aided Civil and Infrastructure Engineering, 37(8), 1027-1043.

Khatibinia, M., Gholami, H., & Labbafi, S. F. (2016). Multi–objective optimization of tuned mass dampers considering soil–structure interaction, International Journal of Optimization in Civil Engineering, 6(4):595-610.

Kennedy J. and Eberhart R., (1995), Particle swarm optimization, Proceedings of ICNN'95-international conference on neural networks, 1942-1948.

Lara-Valencia, L. A., Caicedo, D., & Valencia-Gonzalez, Y. (2021). A novel whale optimization algorithm for the design of tuned mass dampers under earthquake excitations. Applied Sciences, 11(13), 6172.

Liu, Y., Wang, K., Mercan, O., Chen, H., & Tan, P. (2020). Experimental and numerical studies on the optimal design of tuned mass dampers for vibration control of high-rise structures. Engineering Structures, 211, 110486.

Liu, M. Y., Chiang, W. L., Hwang, J. H., & Chu, C. R. (2008). Wind-induced vibration of high-rise building with tuned mass damper including soil–structure interaction. Journal of Wind Engineering and Industrial Aerodynamics, 96(6-7), 1092-1102.

Ogata, K. (2010). Modern Control Systems, United States: Prentice Hall Publications, pp. 669-674.

Salvi, J., Pioldi, F., & Rizzi, E. (2018). Optimum tuned mass dampers under seismic soil-structure interaction. Soil Dynamics and Earthquake Engineering, 114, 576-597.

Yucel, M., Bekdaş, G., Nigdeli, S. M., & Sevgen, S. (2019). Estimation of optimum tuned mass damper parameters via machine learning. Journal of Building Engineering, 26, 100847.

Shahraki, M. A., Kamgar, R., & Heidarzadeh, H. (2023). Assessing the seismic behavior of structures controlled with a novel elastoplastic-tuned mass damper inerter considering the effects of soil-structure interactions. In Structures (Vol. 57, p. 105265). Elsevier.

Thomson, W. (2018). Theory of vibration with applications. CrC Press.

Vanshaj, K., Shukla, A. K., & Shukla, M. (2022). Seismic response on soil–structure interaction of asymmetric plan buildings with active tuned mass dampers. International Journal of Structural Stability and Dynamics, 22(09), 2250102.